RSC Advances

This is an *Accepted Manuscript*, which has been through the Royal Society of Chemistry peer review process and has been accepted for publication.

Accepted Manuscripts are published online shortly after acceptance, before technical editing, formatting and proof reading. Using this free service, authors can make their results available to the community, in citable form, before we publish the edited article. This *Accepted Manuscript* will be replaced by the edited, formatted and paginated article as soon as this is available.

You can find more information about *Accepted Manuscripts* in the Information for Authors.

Please note that technical editing may introduce minor changes to the text and/or graphics, which may alter content. The journal's standard Terms & Conditions and the Ethical guidelines still apply. In no event shall the Royal Society of Chemistry be held responsible for any errors or omissions in this *Accepted Manuscript* or any consequences arising from the use of any information it contains.

ROYAL SOCIETY OF CHEMISTRY

www.rsc.org/advances

Journal Name

RSCPublishing

ARTICLE

New low band gap 2-(4-(trifluoromethyl)phenyl)-1*H*-benzo[*d*]imidazole and benzo[1,2-*c*;4,5-*c*′]bis[1,2,5] thiadiazole based conjugated polymers for organic photovoltaics

Cite this: DOI: 10.1039/x0xx00000x

Received 00th January 2012,
Accepted 00th January 2012

DOI: 10.1039/x0xx00000x

www.rsc.org/

M. G. Murali,[a] Arun D. Rao[a] and Praveen C. Ramamurthy*[a,b]

Two new low band gap D-A structured conjugated polymers, **PBDTTBI** and **PBDTBBT**, based on 2-(4-(trifluoromethyl)phenyl)-1*H*-benzo[*d*]imidazole and benzo[1,2-*c*;4,5-*c*′]bis[1,2,5]thiadiazole acceptor units with benzo[1,2-*b*;3,4-*b*']dithiophene as a donor unit have been designed and synthesized via Stille coupling reaction. The incorporation of benzo[1,2-*c*;4,5-*c*′]bis[1,2,5]thiadiazole unit in PBDTBBT has significantly altered the optical and electrochemical properties of the polymer. The optical band gap estimated from the onset absorption edge are ~1.88 eV and ~1.1 eV, respectively for PBDTTBI and PBDTBBT. It is observed that PBDTBBT exhibited deeper HOMO energy level (−4.08 eV) with strong intramolecular charge transfer interaction. Bulk heterojunction solar cells fabricated with an configuration of ITO/PEDOT:PSS/PBDTBBT:$PC_{71}BM$/Al exhibited a best power conversion efficiency of 0.67 %, with a short circuit current density of 4.9 mA cm^{-2}, an open-circuit voltage of 0.54 V and a fill factor of 25 %.

Introduction

In recent years, research in the area of polymer solar cells (PSCs) have received tremendous attention for the next generation of renewable energy technology over traditional systems due to their light weight, low cost solution fabrication processing, multi-optional synthetic strategies and ease of fabrication.[1–3] In particular, bulk heterojunction (BHJ) structure incorporating organic semiconductor as electron donating and high electron affinity fullerene derivatives such as [6,6]-phenyl-C-butyric acid methyl ester ($PC_{60}BM$ or $PC_{70}BM$) as electron accepting component has proven to be the most successful concept in polymer solar cells.[4,5] However, the commercialization of PSC is mainly limited due to their low power conversion efficiency (PCE). In this view, significant efforts have been made towards improving the efficiency of BHJ polymer solar cells.[6–8]

To date, regioregular poly(3-hexylthiophene) (P3HT) and PCBM based BHJ-PSCs are being extensively studied and showed a significant improvement in the PCEs.[9,10] On the other hand, the P3HT based PSCs exhibit relatively low open circuit voltage (V_{oc} ~0.6) as they can utilize only less than 25 % of solar photons.[3,11] Therefore, to harvest more photons and tune the energy levels of the polymer, several conjugated polymers have been developed.[12–15] With more recently, as a result of better understanding of photon to electron conversion mechanism and the development of new polymeric materials, PCE is reached greater than 10 %.[16]

Common design characteristics for organic semiconductors as a donor material with fullerene derivatives in BHJ solar cells to show excellent photovoltaic properties are, they must possess (i) low optical band gap with broader absorption spectrum such that photons across a broad range of the solar spectrum may be harvested, (ii) low lying highest occupied molecular orbital (HOMO) for high V_{oc} and the short circuit current (J_{sc}), (iii) good crystalline property and solubility for high hole mobility and (iv) appropriate energy levels between polymer and those of fullerene derivatives for efficient charge separation.

In this context, the effective design strategy to obtain narrow band gap polymers is the alternate electron donor (D) and acceptor (A) units along the conjugated polymer backbone.[17–19] Concurrently, it is possible to tune the energy levels of HOMO and band gap of the synthesized (D-A) polymer through proper selection of electron donor and electron acceptor units. Generally, the polymer having "weak donor" unit maintain a low lying HOMO energy level, while a "strong acceptor" segment reduce the band gap via internal charge transfer.[20] In this regard, alkoxy-substituted benzo[1,2-*b*:4,5-*b*′]dithiophene (BDT), a weak electron donor has been demonstrated to be some of the most excellent building blocks for efficient photovoltaic materials.[21] They possess structural

RSC Advances Accepted Manuscript

symmetry and rigid planar system with extended π-electron delocalization.[22] Therefore, BDT based polymers usually display broad absorption and improved charge carrier mobility with deeper HOMO energy level. Many BDT based conjugated polymers with different electron acceptor units such as, 2,1,3-benzothiadiazole (BT)[23], thieno[3,4-*c*]pyrrole-4,6-dione (TPD) [24], thieno[3,4-*b*]thiophene (TT)[25], diketopyrrolopyrrole (DPP)[26] units were used for PSCs.

Benzimidazole as an electron acceptor unit in D-A type conjugated polymer for PSCs is less explored to date. It is interesting building block in the π-conjugated polymer system due to their attractive chemical properties such as photoluminescence and solvatochromism with high thermal stability.[27,28] For instance, alkyl substituted 2*H*-benzo[*d*] imidazole and pentafluorophenyl based conjugated polymers exhibited promising photovoltaic properties.[29-31] In addition, the strong electron withdrawing trifluoromethyl group containing organic molecules have received considerable interest because it can tune the properties of the material such as chemical stability, oxidation stability, thermal stability and solubility.[32,33] Moreover, here the presence of fluorine atom being most electronegative element is expected to stabilize the HOMO and LUMO energy levels, upon introduction of $-CF_3$ group into the conjugated polymer. In the literature, only few examples where $-CF_3$ functional group is introduced into the optoelectronic materials and used for applications such as organic light emitting diodes, organic field-effect transistors and organic solar cells.[34-37].

The benzo[1,2-*c*;4,5-*c*′]bis[1,2,5]thiadiazole (BBT) unit is known to possess a substantial quinoid character and allowing for greater electron delocalization.[38-40] Therefore, BBT a strong electron deficient unit has proved to be an important intermediate compound for the synthesis of low band gap organic materials for organic solar cell and near-infrared (NIR) applications.[41,42]

Herein, we report the synthesis of two new D-A type conjugated polymers (**PBDTTBI** and **PBDTBBT**), based on 2-(4-(trifluoromethyl)phenyl)-1*H*-benzo[*d*]imidazole and benzo [1,2-*c*;4,5-*c*′]bis[1,2,5]thiadiazole acceptor units with benzo [1,2-*b*;3,4-*b*']dithiophene donor unit. Optical, electrochemical and photovoltaic properties of the polymers were further investigated. The best BHJ device, from blending PBDTBBT with $PC_{71}BM$ (1:1, w/w) showed a power conversion efficiency of 0.67 %, with a short-circuit current density of 4.9 mA cm^{-2}, an open-circuit voltage of 0.54 V and a fill factor of 25 %.

Experimental section

Materials and methods

4,7-dibromo-2,1,3-benzothiadiazole (**1**) and thieno[2,3-*f*][1] benzothiophene-4,8-dione (**8**) were synthesized according to the reported procedure.[43,44] o-Phenylenediamine, thiophene-3-carboxylic acid, 4-(trifluoromethyl)benzaldehyde, p-toluene sulfonic acid, tetrakis(triphenylphosphine)palladium(0) and trimethyltin chloride were obtained from Sigma Aldrich chemical company. n-BuLi was purchased from Acros Organics Ltd. Tetrahydrofuran was dried over Na/benzophenone ketyl and freshly distilled. All other reagents were purchased from commercial suppliers and used without further purification. Regioregular P3HT (55 kDa) was purchased from Rieke Metals, $PC_{71}BM$ (>99.5 %) was obtained from Nano-C, ITO coated glass substrates were purchased from Delta Technologies Inc, PEDOT:PSS was from Clevios™ VP AI 4083 and was as used.

^1H and ^{13}C NMR spectra were recorded with a BRUKER NMR spectrometer using TMS as internal reference. Infrared spectra of all the compounds were recorded on a NICOLET 5700 FTIR. UV-Visible absorption spectra were measured using a Perkin Elmer Lambda 35 spectrophotometer. Electrochemical studies of the polymer were carried out using a CH660D CH instrument. Cyclic voltammograms were recorded using a three-electrode cell system, with a glass carbon disk as working electrode, platinum wire as counter electrode and Ag/AgCl electrode as the reference electrode. Gel permeation chromatography (GPC) was used to obtain the molecular weight of the polymers and was determined by Waters make GPC instrument with reference to polystyrene standards and THF as the eluent. Elemental analyses were performed using Thermo Scientific Flash 2000 Organic Elemental Analyzer. Thermogravimetric analysis was carried out using a TGA 2950 (TA instruments-STA 409PC) thermal analyzer. Morphology was characterized using Bruker icon ScanAsyst. The height of the active layer was determined using a Bruker surface profiler (Dektak XT). The current density-voltage (*J-V*) characteristics were measured using Keithley 4200 parameter analyzer. The solar simulator used was Oriel Sol3A Class AAA solar simulator. For the J-V measurements, light intensity of 1kW m^{-2} was employed. The intensities were calibrated using a standard Si solar cell.

Synthesis of monomers and the polymers

The synthetic route for preparing monomers and the polymers are depicted in Scheme 1. The detailed synthetic procedure for the synthesis of monomers and the polymers is as follows.

3,6-dibromobenzene-1,2-diamine (2)

To a solution of 4,7-dibromo-2,1,3-benzothiadiazole **1** (1 g, 3.4 mmol) in 25 ml ethyl alcohol, 2.31 g of sodium borohydride (6.8 mmol) was added in portion wise at 0 ^oC. The resulting mixture was stirred at ambient temperature for 24 h. Then, the reaction mixture was poured into ice cold water and stirred for 1 h. The obtained solid residue was filtered off and washed with water. The product white solid was dried under vacuum. Yield: 80 %. ^1H NMR ($CDCl_3$, 400 MHz), δ (ppm): 6.85 (s, 2H), 3.90 (s, 4 H).

4,7-dibromo-2-(4-(trifluoromethyl)phenyl)-1*H*-benzo[*d*] imidazole (M1)

To a stirred solution of compound **2** (0.5 g, 1.8 mmol) and 4-(trifluoromethyl)benzaldehyde (0.32 g, 1.8 mmol) in 10 ml DMF, 0.06 g of p-toluenesulfonic acid (0.36 mmol) was added.

RSC Advances Accepted Manuscript

This journal is © The Royal Society of Chemistry 2012

The resulting mixture was then heated at 80 ^{o}C for 1 h. After completion of the reaction (progress of the reaction was monitored by TLC), it was poured into a 0.05 M aq. Na_2CO_3 (100 ml). The obtained white precipitate was filtered off and washed with water. The crude product was purified by column chromatography using hexane:ethyl acetate (10:1) as the eluent. The pure product was obtained as white crystal. Yield:80 %. M.P: 254 ^{o}C. ^{1}H NMR ($CDCl_3$, 400 MHz), δ (ppm): 13.59 (s, 1H), 8.56 (d, J=8Hz, 2H), 7.96 (d, J=8Hz, 2H), 7.42 (s, 2H). CHNS: Anal. Calcd. For $C_{14}H_7Br_2F_3N_2$: C, 40.03; H, 1.68; N, 13.57. Found: C, 40.88; H, 1.62; N, 13.22.

4,7-dibromo-5,6-dinitro-2,1,3-benzothiadiazole (3)

Fuming nitric acid (0.75 g, 11.1 mmol) was added drop wise into fuming trifluoromethanesulfonic acid (7.5 g, 50 mmol) in a two necked flask at 0 ^{o}C. Insoluble complex $2CF_3SO_3H/HNO_3$ was produced immediately. To this reaction mixture, 4,7-dibromo-2,1,3-benzothiodiazole **1** (1.25 g, 4.25 mmol) was added in portion wise over a period of 20 min. The reaction was stirred at 50 ^{o}C for 12 h. After completion of the reaction, the reactant was slowly poured into ice cold water and then sodium hydroxide solution was added to neutralize the excess acid. The obtained precipitate was filtered off and washed with water. The crude product was purified by recrystallization using ethanol and obtained as light yellow powder.
Yield: 75 %. ^{13}C NMR ($CDCl_3$, 100 MHz), δ (ppm): 153.59, 145.54, 113.14.

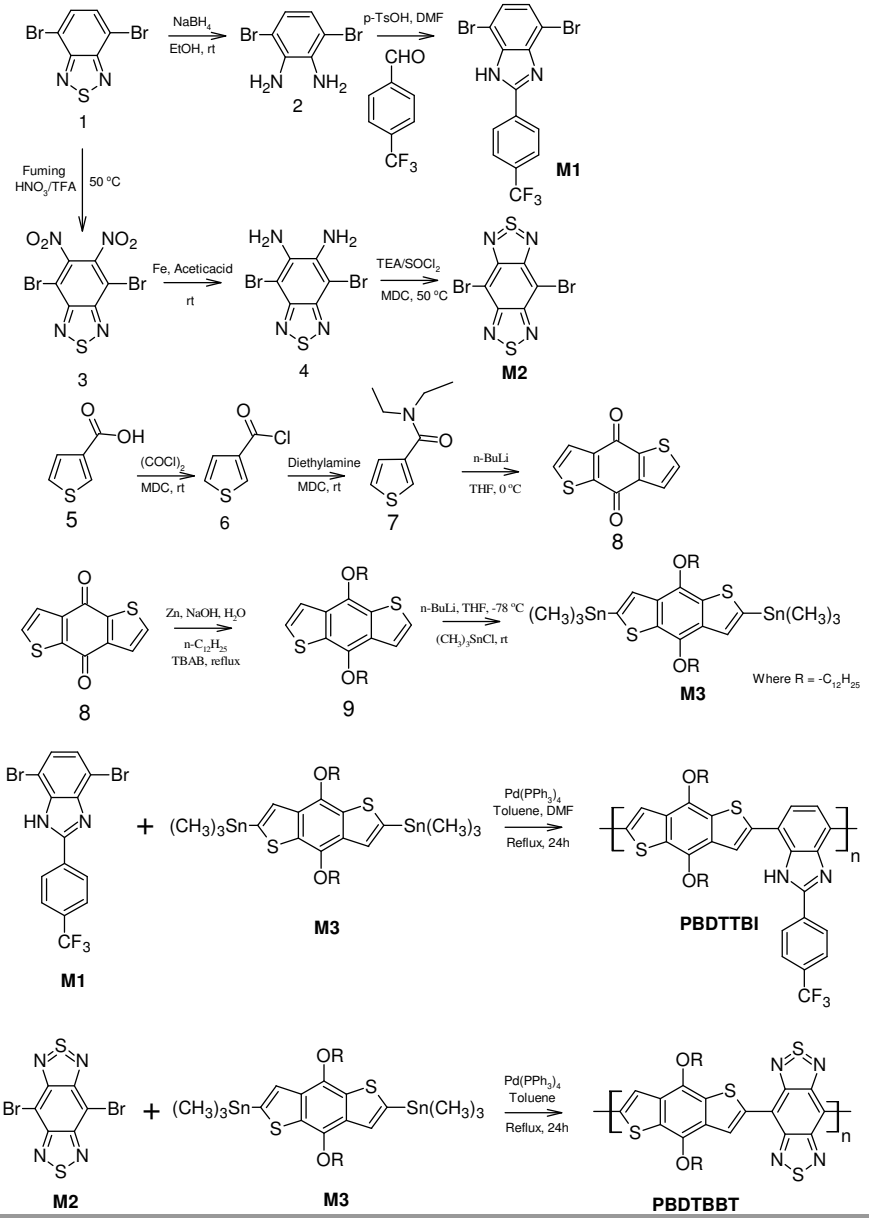

Scheme 1

RSC Advances Accepted Manuscript

Journal Name RSCPublishing

ARTICLE

4,7-dibromo-2,1,3-benzothiadiazole-5,6-diamine (4)

To a stirred solution of compound **3** (1 g, 2.6 mmol) in glacial acetic acid (20 ml), 1.75 g, of fine iron powder (31.25 mmol) was added portion wise at 0 ^{o}C. The reaction mixture was stirred at ambient temperature for 12 h. Then the reactant was poured into ice cold water and the precipitate was filtered off. The obtained product was washed with water, followed by methanol to get yellow solid. Yield: 65 %. ^{1}H NMR ($CDCl_3$, 400 MHz), δ (ppm): 4.49 (br, s, 4H).

4,8-dibromobenzo(1,2-*c*;4,5-*c'*)bis(1,2,5)thiadiazole (M2)

To a stirred solution of compound **4** (0.5 g, 1.54 mmol) in 10 ml of dichloromethane, 0.86 ml of triethylamine (6.17 mmol) was added under inert atmosphere. To this solution, 0.22 ml of thionyl chloride (3.1 mmol) was added drop wise at 0 ^{o}C. The reaction mixture was stirred at 50 ^{o}C for 12 h. After completion of the reaction, the reactant was poured into ice cold water and acidified with concentrated HCl. The obtained solid product was filtered off, washed with water and followed by methanol. The crude product was purified by column chromatography using hexane:ethyl acetate (10:2) as the eluent. The pure product was obtained as dark red solid. Yield: 70 % M.P: 254 ^{o}C. CHNS: Anal. Calcd. For $C_6Br_2N_4S_2$: C, 20.47; N, 15.92; S, 18.22. Found C, 20.66; N, 16.10; S, 18.34.

4,8-didodecyloxybenzo(1,2-*b*;3,4-*b'*)dithiophene (9)

To a stirred solution of compound **8** (1 g, 4.4 mmol) and zinc powder (0.64 g, 9.8 mmol) in 15 ml of water, 4 g of NaOH was added at ambient temperature. The reaction mixture was heated to reflux for 1 h. To this stirred solution, 1-bromdodecane (3.16 ml, 13.2 mmol) and a catalytic amount of tetrabutylammonium bromide (TBAB) were added. The reaction mixture was refluxed for 10 h. After completion of the reaction, the reactant was cooled to ambient temperature and poured into ice cold water. The aqueous layer was extracted with diethyl ether. The organic phase was dried over anhydrous $MgSO_4$ and concentrated. Finally, the crude product was purified by column chromatography using hexane as the eluent. The pure product was obtained as white solid. Yield: 80 %. ^{1}H NMR ($CDCl_3$, 400 MHz), δ (ppm): 7.47 (d, 2H), 7.36 (d, 2H), 4.27 (t, 4H), 1.87(quintuple, 4H), 1.56 (m, 4H), 1.42-1.27 (m, 32H), 0.89 (t, 6H).

2,6-bis(trimethyltin)-4,8-didodecyloxybenzo[1,2-*b*;3,4-*b'*]di thiophene (M3)

To a stirred solution of compound **9** (0.5 g, 0.9 mmol) in 10 ml of freshly distilled THF, 1.23 ml of n-butyllithium (1.98 mmol, 1.6 M in *n*-hexane) was added drop wise at –78 ^{o}C under inert atmosphere. The reactant was stirred at same temperature for 1 h. To this stirred solution, 1.98 ml of trimethyltin chloride (1.98 mmol, 1 M in n-hexane) was added in one portion. The reaction mixture was stirred at ambient temperature for 12 h. Then, it was poured into water and extracted with diethyl ether. The organic phase was washed with water three times, dried over anhydrous $MgSO_4$ and concentrated. The crude product was recrystallized using ethyl alcohol three times to obtain colorless needle crystal. Yield: 75 %. ^{1}H NMR ($CDCl_3$, 400 MHz), δ (ppm): 7.45 (s, 2H), 4.22 (t, 4H), 1.86 (quintuple, 4H), 1.55 (m, 4H), 1.54 (m, 4H), 1.40-1.25 (m, 32H), 0.89 (t, 6H), 0.44 (s, 18 H).

General procedure for the synthesis of polymers using Stille coupling reaction

Monomer **M1** (105 mg, 0.25 mmol) and monomer **M3** (221 mg, 0.25 mmol) were dissolved in 10 ml of toluene and 2 ml of DMF. The stirred solution was flushed with nitrogen for 20 min and then $Pd(PPh_3)_4$ (15 mg) was added. The reaction mixture was again flushed with nitrogen for 20 min and it was refluxed for 24 h under nitrogen atmosphere. The reactant was cooled to ambient temperature and the polymer was precipitated by addition of 100 mL of methanol and filtered off. The crude polymer was subjected to soxhlet extraction with methanol, hexane and chloroform. The polymer was recovered as a solid sample from the chloroform fraction by rotary evaporation. The red colored polymer (PBDTTBI) was dried under vacuum at 40 ^{o}C for 12 h. Similarly, the polymer PBDTBBT was synthesized according to the above mentioned procedure. Yield: 40–60 %. The polymer PBDTTBI was partially soluble in chloroform and DMSO-d6 solvent so we have characterized it by FTIR.

PBDTTBI: FTIR, $\sqrt{}$ (cm^{-1}): 3435 (-NH), 2924 and 2853 (-C-H), 1619 (-C=C-), 1599 (-C-N), 1428, 1359, 1323, 1168 (-C-O-), 1127, 1062, 846.

PBDTBBT: ^{1}H NMR ($CDCl_3$, 400 MHz), δ (ppm): 7.50 (s, 2H), 4.3 (t, 4H), 1.85 (quintuple, 4H), 1.52 (m, 4H), 1.40-1.28 (m, 32H), 0.86 (t, 6H).

Fabrication and characterization of photovoltaic devices

Initially, the ITO-coated glass substrates (70–150 Ωsq^{-1}) were consecutively cleaned in isopropyl alcohol, acetone and soap solution under sonication for ~5 min. The cleaned substrate was then washed with deionized water and subsequently dried over nitrogen gas. Cleaned ITO substrate was UV-ozone treated and PEDOT:PSS was spin coated at 3000 rpm for 60 sec. Finally, the spin coated samples were annealed at 110

RSC Advances Accepted Manuscript

°C for 15 min before being transferred into a glove box with less than 1 ppm of oxygen and moisture.

Inside the glove box, solution of binary blend PBDTTBI:$PC_{71}BM$ and PBDTBBT:$PC_{71}BM$ with a 1:1 weight ratio, 7.5 mg of each material was dissolved in 1 ml of 1,2-dichlorobenzene. The obtained blend solution was stirred at ambient temperature for ~12 h. The blend solution was spin-coated on transferred ITO substrate at 1000 rpm for 60 sec. The fabricated active layer was annealed at 150 °C for 15 min on a hot plate. This aids in the phase separation of polymer and PCBM, which in turn helps in establishing a well functioning bulk heterojunction. The active layers of all the devices had a comparable thickness in the range of about 200 nm as determined by profilometer. Finally, the cathode aluminum layer (100 nm) was deposited by thermal evaporation under vacuum (8×10^{-7} torr). The fabricated solar cell has an active area of 9 mm^2.

Results and discussion

Monomer and polymer synthesis

The synthetic route of polymers **PBDTTBI** and **PBDTBBT** are depicted in Scheme 1. The compound 3,6-dibromobenzene-1,2-diamine (**2**) was synthesized by treating 4,7-dibromo-2,1,3-benzothiadiazole (**1**) with sodium borohydride at 0 °C. The obtained product **2** was taken as such for the next without any further purification.

To prepare CF_3 functionalized monomer **M1**, the compound **2** was reacted with 4-(trifluoromethyl)benzaldehyde in the presence of p-TsOH as the organocatalyst in DMF at 80 °C for 1 h. Synthesis of 4,8-dibromobenzo[1,2-*c*;4,5-*c*']bis[l,2,5] thiadiazole monomer (**M2**) was achieved via a three step procedure. Initially, nitration reaction was carried out to compound **1** using fuming HNO_3/CF_3SO_3H at 50 °C to yield dinitro compound **3**. Further, the reduction of compound **3** using iron powder in acetic acid afforded the compound **4** with a good yield. Finally, cyclization reaction was performed to compound **4** using triethylamine and thionyl chloride in dichloromethane at 50 °C afforded the monomer **M2**.

To synthesize thieno[2,3-*f*][1]benzothiophene-4,8-dione (**8**), initially the compound thiophene-3-carboxylic acid (**5**) was converted into its acid chloride **6** using oxalyl chloride. Then the compound **6** was reacted with diethylamine in dichloromethane afforded the *N*,*N*-diethylthiophene-3-carboxamide (**7**). Compound **7** was cyclized using n-BuLi in anhydrous THF under inert atmosphere to obtain compound **8**. Synthesis of monomer **M3** involves two steps. First, alkylation reaction was carried out by treating compound **8** with 1-bromododecane in the presence of zinc, NaOH and a catalytic amount of TBAB in water under reflux condition afforded the compound **9**. Stannylated monomer **M3** was prepared in a simple and straightforward reaction using trimethyltin chloride and n-BuLi in freshly distilled THF at −78 °C under inert atmosphere. The target D-A type polymers **PBDTTBI** and **PBDTBBT** were prepared via a Pd(0)-mediated Stille coupling reaction between brominated monomers (**M1** or **M2**) and the bis(trimethylstannyl) substituted monomer **M3** in good yield (40–60 %). The crude polymers were soxhlet-extracted with methanol, hexane and chloroform in sequence. Finally, the titled polymers were recovered by reprecipitation from their concentrated chloroform solutions using methanol. The resulting polymers showed good solubility in organic solvents such as chlorobenzene, THF, 1,2-dichlorobenzene etc. The molecular weight and polydispersity index (PDI) of the polymers were measured by gel permeation chromatography (GPC) using polystyrene as the standard and THF as the eluent. The number-average molecular weight (M_n) = 11400 and PDI = 2.8 for **PBDTTBI**, M_n = 18200 and PDI = 2.4 for **PBDTBBT**.

The thermal properties of the polymers were investigated using thermal gravimetric analysis (TGA) and were carried out under nitrogen atmosphere at a heating rate of 10 °C min^{-1}. As shown in the Fig. 1, the polymers showed good thermal stability with onset decomposition temperature (5 % weight) is ~310 °C and ~275 °C, respectively for PBDTTBI and PBDTBBT. Further, an abrupt weight loss was observed as the temperature was increased above their onset decomposition temperature, indicating the decomposition of the polymer backbone.

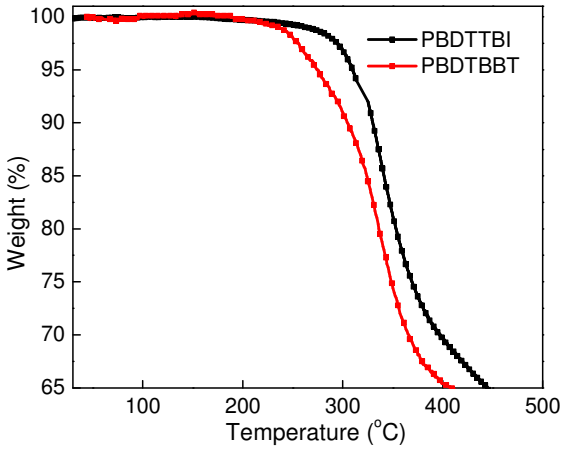

Fig. 1 TGA plot of **PBDTTBI** and **PBDTBBT** with a heating rate of 10 °C/min under N_2 atmosphere

Optical properties

UV-Vis absorption spectroscopy was used to investigate the photophysical properties of the polymer. The absorption spectra of the polymers in dilute chlorobenzene solution and as spin coated film on glass plates are as shown in the Fig. 2. The polymer PBDTTBI exhibited an absorption profile with two major peaks with slightly different absorption maxima and which could be attributed to the π–π* transition in the polymer backbone. In the solution form, PBDTTBI displayed absorption bands at 510 and 550 nm, whereas it showed absorption peaks at 514 and 560 nm in their film state (Fig. 2a). The observed slight red shift and broader absorption band for PBDTTBI film as compared to its solution state could be credited to their better planarity and stronger electronic interaction between the individual polymer chains.

RSC Advances Accepted Manuscript

In case of polymer PBDTBBT, two characteristic absorption bands were observed at 384 and ~520–1100 nm (Fig. 2b) The observed band at the shorter wavelength region could be due to the π–π* transition state from the BDT repeating unit in the polymer chain[45,41], whereas the peak in the longer wavelength region could be attributed to the strong intramolecular charge transfer interaction between electron donor BDT and acceptor BBT unit in the polymer[46]. Optical band gap (E_g^{opt}), defined by the onset absorption spectra of the polymer film was found to be ~1.88 and ~1.1 eV, respectively for PBDTTBI and PBDTBBT. As s result of large quinoid structure of BBT molecule in the D-A-D segment of PBDTBBT, it showed a narrow band gap (~1.1 eV) in comparison to that of PBDTTBI.[47-49] Moreover, the absorption

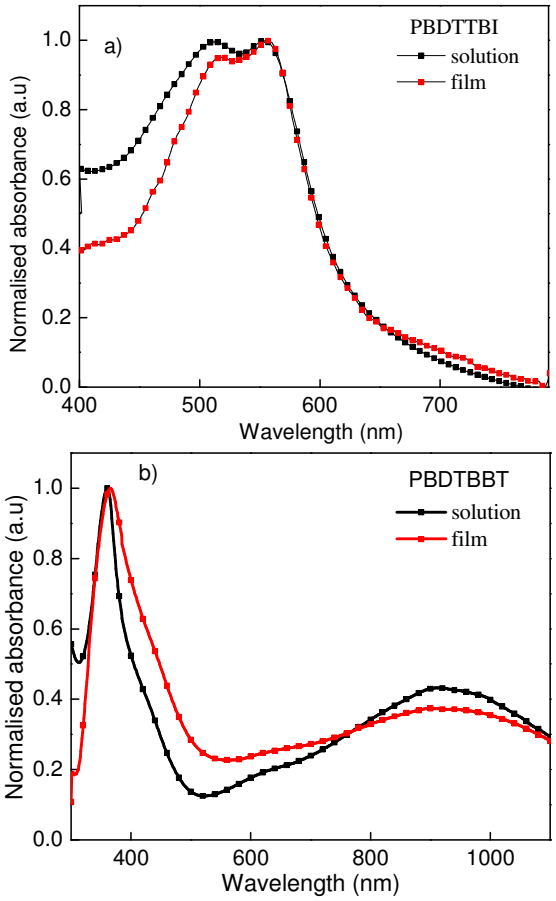

Fig. 2 Optical absorption spectra of a) **PBDTTBI** and b) **PBDTBBT** both in solution and thin film

region of PBDTBBT film in the longer wavelength region was broader as compare to its solution state presumably due to the π-stacking effect. It was observed that absorption spectrum of PBDTBBT is almost completely covered the entire near–IR region, which further demonstrates the polymer can absorb most of the photons of the solar spectrum with the lowest energy. Overall these results indicate that polymer PBDTBBT is expected to show improved photovoltaic performance in comparison to that of PBDTTBI.

Electrochemical properties

Electrochemical cyclic voltammetry (CV) was employed to determine the HOMO and LUMO energy levels of the polymer, which were estimated from the point where the current signal of oxidation and reduction potential start to deviate from the baseline.[50] Cyclic voltammograms of polymer were recorded by spin coating the polymer solution on glassy carbon (GC) disk electrode with 0.1 M tetrabutylammonium hexafluorophosphate in CH_3CN as the electrolyte at a scan rate of 100 mV s^{-1}. For calibration, the redox potential of ferrocene/ferrocenium (Fc/Fc+) was measured under the same conditions and it was located at 0.11 V to the Ag/AgCl electrode. It was assumed that the redox potential of Fc/Fc+ has an absolute energy level of −4.80 eV to vacuum.[51] The HOMO and LUMO energy levels of the polymer were calculated according to the following equation[52]

$$E_{HOMO} = -(E_{on}^{ox} - E_{Fc/Fc^+} + 4.80)\ eV$$

$$E_{LUMO} = -(E_{on}^{red} - E_{Fc/Fc^+} + 4.80)\ eV$$

As shown in the Fig. 3a, PBDTTBI exhibited p-doping process and the onset oxidation potential is observed at 0.31 V vs Ag/Ag^+. Nevertheless, polymer did not show any sharp potential for reduction process. Therefore, the LUMO value of the polymer was calculated using their optical band gap [$E_{LUMO} = E_{HOMO} - E_g^{opt}$] eV. The calculated HOMO and LUMO levels were found to be −5.0 and −3.12 eV, respectively.

The onset oxidation and reduction potential values of PBDTBBT were estimated to be 0.68 and -0.63 V, respectively (Fig. 3b.). The HOMO and LUMO energy levels were determined to be −5.37 and −4.06 eV, respectively. The observed deeper HOMO and LUMO energy level for PBDTBBT could be resulted from their strong electron withdrawing BBT unit in their back bone. The electrochemical band gap (E_g^{cv}) of the polymers were ~1.88 and ~1.31 eV, respectively for PBDTTBI and PBDTBBT. The estimated values were consistent with the optical band gap obtained from UV-Vis studies and the values are summarized in Table 1. The energy levels of the polymer and $PC_{71}BM$ as calculated from electrochemistry are summarized in Fig. 4.

Table 1 Summary of optical and electrochemical properties of polymers

Polymer	λ_{abs} solution (nm)	λ_{abs} film (nm)	λ_{onset} film (nm)	E_g^{opt} (eV)	HOMO (eV)	LUMO (eV)
PBDTTBI	510/ 550	514/ 560	660	1.88	-5.0	-3.12
PBDTBBT	361/ 911	368/ 911	1128	1.1	-5.37	-4.06

It is known that the open circuit voltage V_{oc} is one of main contributor in estimating the efficiency of PSCs. The V_{oc} is directly related with the difference between HOMO energy level of electron donor, conjugated polymer, and the LUMO

RSC Advances Accepted Manuscript

This journal is © The Royal Society of Chemistry 2012

energy level of the electron acceptor, fullerene derivatives. The obtained deep HOMO energy level of PBDTBBT (–5.37 eV) was desired for achieving a higher V_{oc} in the BHJ PSCs and made this a promising candidate for use as electron donor material. It is obvious that the LUMO energy level of the D-A type polymer is strongly dependent upon the electron accepting unit (A). Here the polymer PBDTBBT showed a deeper LUMO level and is quiet close to that of PCBM with an offset of 0.1–0.2 V, which indicates that the electron transfer between polymer to PCBM may not be so effective since it is generally should be ~0.3–0.4 eV.[53-54]

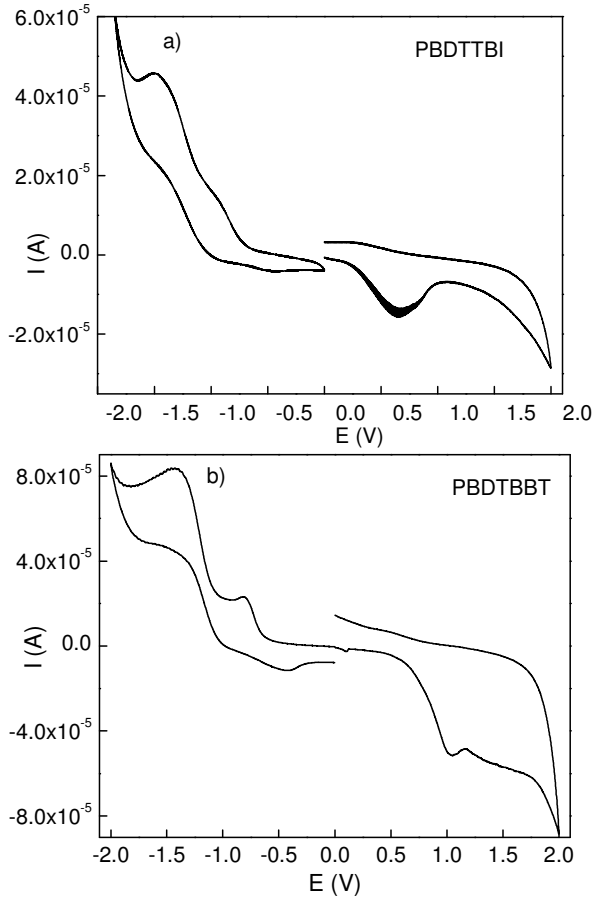

Fig. 3 Cyclic voltammogram of a) **PBDTTBI** and b) **PBDTBBT** film on glassy carbon electrode in 0.1 mol/L Bu_4NPF_6, CH_3CN solution

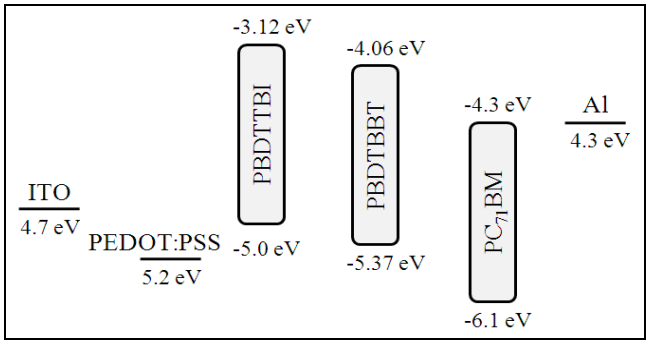

Fig. 4 Energy levels [eV] of the electrodes, PBDTTBI, PBDTBBT and PCBM

Molecular orbital calculations

To investigate the electron distribution of the frontier orbitals of the polymer, density functional theory (DFT) calculations were performed at the B3LYP/6-311G (d) level. The long alkyl side chains in the repeating unit of the polymer were replaced with methyl group and their electron density distribution was estimated. The optimized geometry of polymer PBDTTBI and PBDTBBT is as shown in Fig. 5 and 6. In both the polymers, the electron density of HOMO is distributed along the entire π–conjugated system, indicates that HOMO energy level is affected by both electron donor and acceptor units (Fig. 5b and 6b). The localization of the electron density of LUMO in PBDTTBI is more pronounced on the benzo[*d*]imidazole ring with trifluoromethyl substitution (Fig. 5c).

In case of PBDTBBT, the electron density of LUMO is distributed on thiadiazole ring (Fig. 6c). The theoretically predicted HOMO/LUMO levels of the polymers were found to be –4.89/–2.99 and –4.62/–4.16 eV, respectively for PBDTTBI and PBDTBBT. The present DFT computed predicted HOMO/LUMO values of the polymer were slightly differ than their experimentally calculated values. The observed trend could be due to various effects such as conformational order in bulk state, effect of solvent and electrolyte which were not taken into account.[37] The strong electron withdrawing thiadiazole ring based polymer PBDTBBT exhibited lowest LUMO value, which follows a similar trend observed experimentally.

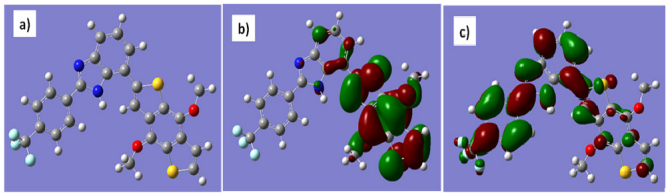

Fig. 5 The optimized geometries of **PBDTTBI** (a) and their HOMO (b), LUMO (c) by DFT methods at the B3LYP/6-311G level

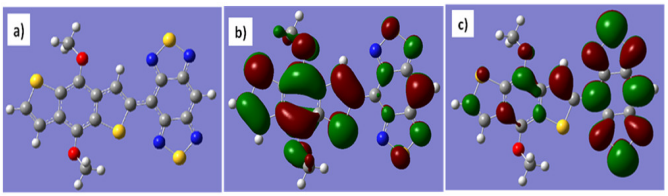

Fig. 6 The optimized geometries of **PBDTBBT** (a) and their HOMO (b), LUMO (c) by DFT methods at the B3LYP/6-311G level

Photovoltaic properties and active layer morphology

The photovoltaic properties of the polymers were investigated in BHJ solar cell devices and the device structure is ITO/PEDOT:PSS(~50 nm)/polymer:$PC_{71}BM$/Al (100 nm). The devices were measured under AM 1.5 G (100 mW cm^{-2}) illumination. The current density–voltage (*J–V*) characteristics of the BHJ solar cell devices are displayed in Fig. 7 and the photovoltaic properties are summarized in Table 2. The device based on PBDTTBI:$PC_{71}BM$ (1:1, w/w) exhibited a PCE of

RSC Advances Accepted Manuscript

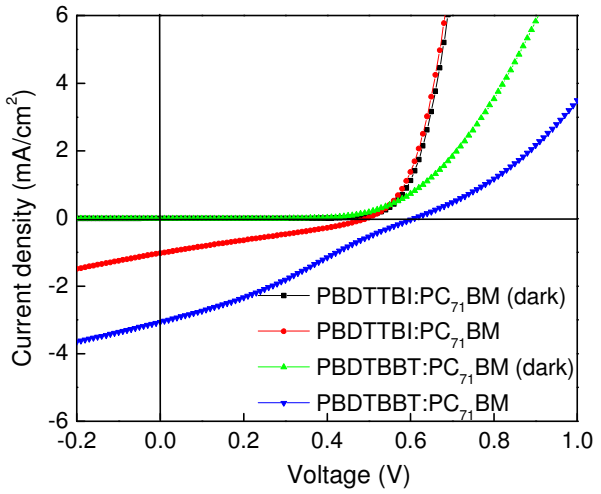

Fig. 7 *J–V* characteristics of **PBDTTBI:PC$_{71}$BM** and **PBDTBBT:PC$_{71}$BM** (1:1, w/w) blend films

0.14 % with a J_{sc} of 1.1 mA cm^{-2}, V_{oc} of 0.5 V and a FF of 27.6 %. The blend film PBDTBBT:PC$_{71}$BM (1:1, w/w) having broad UV-Vis absorption spectra showed a moderately high PCE of 0.67 % with a J_{sc} of 4.9 mA cm^{-2}, V_{oc} of 0.54 V and a FF 25.0 %. The V_{oc} of the PBDTBBT:PC$_{71}$BM device was relatively high, which could be attributed to their low lying HOMO energy level. In addition, the polymer PBDTBBT absorbed strongly in visible and the NIR region, which yielded in moderately high J_{sc} value for the resulting device. At higher content of PC$_{71}$BM in the active layer, the polymer and PCBM phases are separated into larger domains and also the domain sizes increases with increase in the PCBM fraction. As a result, this reduces the heterojunction interface area for exciton dissociation and consequently led to the low J_{sc} value and poor device performance.[55] Here also similar trend was observed for blend films at higher PCBM content (1:1.5, 1:2 w/w). This observation was further supported by the morphological studies.

The morphology of the active layer is important for the performance of BHJ solar cells. To investigate the morphology of the blend films, atomic force microscopy (AFM) experiments were performed. The polymer:PC$_{71}$BM blend films with different weight ratios were spin coated from 1,2-dichlorobenzene solution onto the glass/ITO/PEDOT:PSS substrate and the AFM images are as shown in Fig. 8. The surface roughness (R_{RMS}) of the AFM topographic images was ~5.15 and ~0.53 nm, respectively for PBDTTBI:PC$_{71}$BM (1:1, w/w) and PBDTBBT:PC$_{71}$BM (1:1, w/w) blends. Nevertheless, the phase images of the blend films did not show uniform nano-scaled phase separated interpenetrating D-A network. This indicates that excessive phase separation may happen, which can limit device performance. Although polymers exhibited broad absorption spectra with deep HOMO energy levels, the observed low PCEs of polymer solar cells could be resulted from poor quality and homogeneity of the blend films.[56-58] Moreover, the observed low FF and poor device performance of the polymer solar cell fabricated on the ITO coated glass plate could be due to their high resistance. Therefore, it is believed that device engineering such as annealing optimization, additive and device architecture optimization can enhance the device performance.

Table 2 Summary of PSCs performances of devices based on PBDTTBI: PC$_{71}$BM and PBDTBBT:PC$_{71}$BM

Polymer	J_{SC} (mA cm^{-2})	V_{OC} (V)	FF (%)	Efficiency (%)
PBDTTBI (1:1, w/w)	1.1	0.5	27.6	0.14
PBDTTBI (1:1.5, w/w)	0.43	0.48	26	0.06
PBDTTBI (1:2, w/w)	0.1	0.47	27	0.01
PBDTBBT (1:1, w/w)	4.9	0.54	25	0.67
PBDTBBT (1:1.5, w/w)	3.6	0.6	30	0.64
PBDTBBT (1:2, w/w)	2.44	0.6	28	0.43

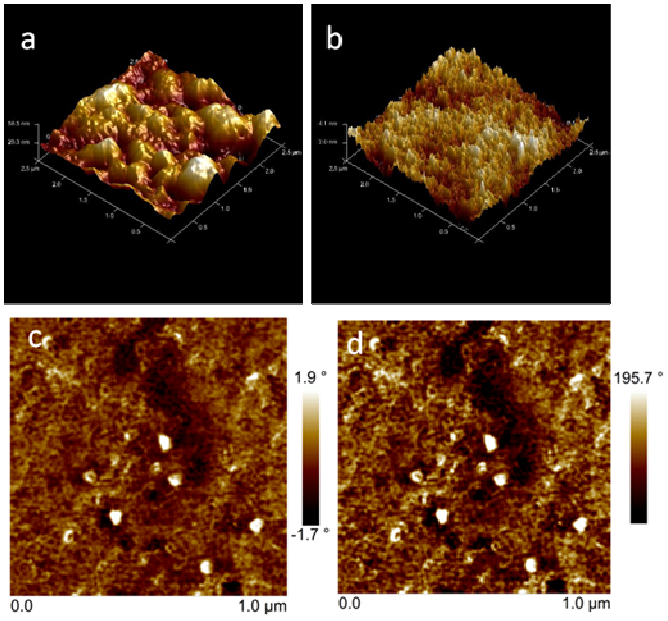

Fig. 8 AFM height images of polymer:PC$_{71}$BM blend films on ITO/PEDOT:PSS: (a) PBDTTBI:PC$_{71}$BM (b) PBDTBBT:PC$_{71}$BM; AFM phase images of polymer:PC$_{71}$BM blend films on ITO/PEDOT:PSS: (c) PBDTTBI:PC$_{71}$BM (d) PBDTBBT:PC$_{71}$BM

Conclusions

In summary, we have designed and synthesized two novel D-A type polymers (**PBDTTBI** and **PBDTBBT**) containing common donor segment (BDT) with 2-(4-(trifluoromethyl) phenyl)-1*H*-benzo[*d*]imidazole and benzo[1,2-*c*;4,5-*c*′]bis [1,2,5]thiadiazole acceptor units for organic solar cell applications. The polymer PBDTBBT showed a narrow band gap and broader absorption spectra with a deeper HOMO energy level. The photovoltaic properties of polymers were investigated in typical BHJ devices using PC$_{71}$BM as an acceptor. A moderately high PCE of 0.64 %, with a short circuit current density of 4.9 mA cm^{-2}, open-circuit voltage of 0.54 V, and a fill factor of 25 % was achieved for PBDTBBT, could be as a benefit of their broad absorption spectra. These studies demonstrate that introducing BBT unit having large quinoid structure in D-A-D type polymer is an effective design

RSC Advances Accepted Manuscript

This journal is © The Royal Society of Chemistry 2012

strategy to achieve low band gap with broad absorption for PSC applications.

Acknowledgements

This work is based upon work supported in part under the US-India Partnership to Advance Clean Energy-Research (PACE-R) for the Solar Energy Research Institute for India and the United States (SERIIUS), funded jointly by the U.S. Department of Energy (Office of Science, Office of Basic Energy Sciences, and Energy Efficiency and Renewable Energy, Solar Energy Technology Program, under Subcontract DE-AC36-08GO28308 to the National Renewable Energy Laboratory, Golden, Colorado) and the Government of India, through the Department of Science and Technology under Subcontract IUSSTF/JCERDC-SERIIUS/2012 dated 22nd Nov. 2012.

Notes and references

[a]Department of Materials Engineering, [b]Center for Nanoscience and Engineering, Indian Institute of Science, Bangalore, India. Fax: +91-80-2360-0472; Tel: +91-80-2293-2627; E-Mail: praveen@materials.iisc.ernet.in

1. G. Yu, J. Gao, J. C. Hummelen, F. Wudl, and A. J. Heeger, *Science*, 1995, **270**, 1789–1791.
2. M. M. Wienk, J. M. Kroon, W. J. H. Verhees, J. Knol, J. C. Hummelen, P. A. van Hal, and R. A. J. Janssen, *Angewandte Chemie International Edition*, 2003, **42**, 3371–3375.
3. G. Dennler, M. C. Scharber, and C. J. Brabec, *Advanced Materials*, 2009, **21**, 1323–1338.
4. K. Vandewal, S. Himmelberger, and A. Salleo, *Macromolecules*, 2013, **46**, 6379–6387.
5. S. Kouijzer, J. J. Michels, M. van den Berg, V. S. Gevaerts, M. Turbiez, M. M. Wienk, and R. A. J. Janssen, *J. Am. Chem. Soc.*, 2013, **135**, 12057–12067.
6. Z. He, C. Zhong, X. Huang, W.-Y. Wong, H. Wu, L. Chen, S. Su, and Y. Cao, *Advanced Materials*, 2011, **23**, 4636–4643.
7. L. Dou, J. You, J. Yang, C.-C. Chen, Y. He, S. Murase, T. Moriarty, K. Emery, G. Li, and Y. Yang, *Nat Photon*, 2012, **6**, 180–185.
8. Z. He, C. Zhong, S. Su, M. Xu, H. Wu, and Y. Cao, *Nat Photon*, 2012, **6**, 591–595.
9. M. D. McGehee and M. A. Topinka, *Nat Mater*, 2006, **5**, 675–676.
10. H. Hoppe, M. Niggemann, C. Winder, J. Kraut, R. Hiesgen, A. Hinsch, D. Meissner, and N. S. Sariciftci, *Advanced Functional Materials*, 2004, **14**, 1005–1011.
11. C. J. Brabec, S. Gowrisanker, J. J. M. Halls, D. Laird, S. Jia, and S. P. Williams, *Advanced Materials*, 2010, **22**, 3839–3856.
12. Y. Li, *Accounts of Chemical Research*, 2012, **45**, 723–733.
13. H.-Y. Chen, J. Hou, S. Zhang, Y. Liang, G. Yang, Y. Yang, L. Yu, Y. Wu, and G. Li, *Nat Photon*, 2009, **3**, 649–653.
14. L. Dou, J. Gao, E. Richard, J. You, C.-C. Chen, K. C. Cha, Y. He, G. Li, and Y. Yang, *Journal of the American Chemical Society*, 2012, **134**, 10071–10079.
15. T.-Y. Chu, J. Lu, S. Beaupré, Y. Zhang, J.-R. Pouliot, S. Wakim, J. Zhou, M. Leclerc, Z. Li, J. Ding, and Y. Tao, *Journal of the American Chemical Society*, 2011, **133**, 4250–4253.
16. J. You, L. Dou, K. Yoshimura, T. Kato, K. Ohya, T. Moriarty, K. Emery, C.-C. Chen, J. Gao, G. Li, and Y. Yang, *Nat Commun*, 2013, **4**, 1446.
17. J. Roncali, *J. Mater. Chem.*, 1999, **9**, 1875–1893.
18. A. Ajayaghosh, *Chem. Soc. Rev.*, 2003, **32**, 181–191.
19. E. E. Havinga, W. ten Hoeve, and H. Wynberg, *Synthetic Metals*, 1993, **55**, 299 – 306.
20. H. Zhou, L. Yang, S. Stoneking, and W. You, *ACS Applied Materials & Interfaces*, 2010, **2**, 1377–1383.
21. J.-M. Jiang, H.-K. Lin, Y.-C. Lin, H.-C. Chen, S.-C. Lan, C.-K. Chang, and K.-H. Wei, *Macromolecules*, 2014, **47**, 70–78.
22. H. Pan, Y. Li, Y. Wu, P. Liu, B. S. Ong, S. Zhu, and G. Xu, *Journal of the American Chemical Society*, 2007, **129**, 4112–4113.
23. Y. Zhang, L. Gao, C. He, Q. Sun, and Y. Li, *Polym. Chem.*, 2013, **4**, 1474–1481.
24. H. Zhong, Z. Li, F. Deledalle, E. C. Fregoso, M. Shahid, Z. Fei, C. B. Nielsen, N. Yaacobi-Gross, S. Rossbauer, T. D. Anthopoulos, J. R. Durrant, and M. Heeney, *Journal of the American Chemical Society*, 2013, **135**, 2040–2043.
25. W. Li, W. S. C. Roelofs, M. M. Wienk, and R. A. J. Janssen, *Journal of the American Chemical Society*, 2012, **134**, 13787–13795.
26. L. Huo, S. Zhang, X. Guo, F. Xu, Y. Li, and J. Hou, *Angewandte Chemie International Edition*, 2011, **50**, 9697–9702.
27. J. Catalan, R. M. Claramunt, J. Elguero, J. Laynez, M. Menendez, F. Anvia, J. H. Quian, M. Taagepera, and R. W. Taft, *Journal of the American Chemical Society*, 1988, **110**, 4105–4111.
28. H. Hayashi and T. Yamamoto, *Macromolecules*, 1998, **31**, 6063–6070.
29. S. Song, Y. Jin, S. H. Park, S. Cho, I. Kim, K. Lee, A. J. Heeger, and H. Suh, *J. Mater. Chem.*, 2010, **20**, 6517–6523.
30. M. Neophytou, H. A. Ioannidou, T. A. Ioannou, C. L. Chochos, S. P. Economopoulos, P. A. Koutentis, G. Itskos, and S. A. Choulis, *Polym. Chem.*, 2012, **3**, 2236–2243.
31. H. Zhu, H. Tong, Y. Gong, S. Shao, C. Deng, W. Z. Yuan, and Y. Zhang, *Journal of Polymer Science Part A: Polymer Chemistry*, 2012, **50**, 2172–2181.
32. P. Deng, Z. Wu, K. Cao, Q. Zhang, B. Sun, and S. R. Marder, *Polym. Chem.*, 2013, **4**, 5275–5282.
33. P. Kirsch, in *Modern Fluoroorganic Chemistry*, Wiley-VCH Verlag GmbH & Co. KGaA, 2005, pp. 203–277.
34. B. Zhang, G. Tan, C.-S. Lam, B. Yao, C.-L. Ho, L. Liu, Z. Xie, W.-Y. Wong, J. Ding, and L. Wang, *Advanced Materials*, 2012, **24**, 1873–1877.
35. S. Ando, R. Murakami, J. Nishida, H. Tada, Y. Inoue, S. Tokito, and Y. Yamashita, *Journal of the American Chemical Society*, 2005, **127**, 14996–14997.
36. P. Deng, Y. Yan, S.-D. Wang, and Q. Zhang, *Chem. Commun.*, 2012, **48**, 2591–2593.
37. P. Sonar, G.-M. Ng, T. T. Lin, A. Dodabalapur, and Z.-K. Chen, *J. Mater. Chem.*, 2010, **20**, 3626–3636.
38. Y. Yamashita, K. Ono, M. Tomura, and S. Tanaka, *Tetrahedron*, 1997, **53**, 10169 – 10178.
39. T. L. Tam, H. Li, F. Wei, K. J. Tan, C. Kloc, Y. M. Lam, S. G. Mhaisalkar, and A. C. Grimsdale, *Organic Letters*, 2010, **12**, 3340–3343.

RSC Advances Accepted Manuscript

40. H. Li, T. L. Tam, Y. M. Lam, S. G. Mhaisalkar, and A. C. Grimsdale, *Organic Letters*, 2011, **13**, 46–49.
41. M. L. Keshtov, D. V. Marochkin, V. S. Kochurov, A. R. Khokhlov, E. N. Koukaras, and G. D. Sharma, *J. Mater. Chem. A*, 2014, **2**, 155–171.
42. X. Li, A. Liu, S. Xun, W. Qiao, X. Wan, and Z. Y. Wang, *Organic Letters*, 2008, **10**, 3785–3787.
43. K. Ranjith, S. K. Swathi, P. Kumar, and P. C. Ramamurthy, *Solar Energy Materials and Solar Cells*, 2012, **98**, 448 – 454.
44. J. Hou, M.-H. Park, S. Zhang, Y. Yao, L.-M. Chen, J.-H. Li, and Y. Yang, *Macromolecules*, 2008, **41**, 6012–6018.
45. J. Hai, W. Yu, B. Zhao, Y. Li, L. Yin, E. Zhu, L. Bian, J. Zhang, H. Wu, and W. Tang, *Polym. Chem.*, 2014, **5**, 1163–1172.
46. Y. Zhu, R. D. Champion, and S. A. Jenekhe, *Macromolecules*, 2006, **39**, 8712–8719.
47. C. Kitamura, S. Tanaka, and Y. Yamashita, *Chemistry of Materials*, 1996, **8**, 570–578.
48. K. Ono, S. Tanaka, and Y. Yamashita, *Angewandte Chemie International Edition in English*, 1994, **33**, 1977–1979.
49. J. L. Brédas, *The Journal of Chemical Physics*, 1985, **82**, 3808–3811.
50. Y. Li, Y. Cao, J. Gao, D. Wang, G. Yu, and A. J. Heeger, *Synthetic Metals*, 1999, **99**, 243 – 248.
51. J. Pommerehne, H. Vestweber, W. Guss, R. F. Mahrt, H. Bässler, M. Porsch, and J. Daub, *Advanced Materials*, 1995, **7**, 551–554.
52. Q. Sun, H. Wang, C. Yang, and Y. Li, *J. Mater. Chem.*, 2003, **13**, 800–806.
53. J.-L. Brédas, D. Beljonne, V. Coropceanu, and J. Cornil, *Chemical Reviews*, 2004, **104**, 4971–5004.
54. B. C. Thompson and J. M. J. Fréchet, *Angewandte Chemie International Edition*, 2008, **47**, 58–77.
55. K. Shibasaki, K. Tabata, Y. Yamamoto, T. Yasuda and M. Kijima, *Macromolecules*, 2014, **47**, 4987–4993.
56. D. Zha, L. Chen, F. Wu, H. Wang, and Y. Chen, *Polym. Chem.*, 2013, **4**, 2480–2488.
57. X.-D. Dang, A. B. Tamayo, J. Seo, C. V. Hoven, B. Walker, and T.-Q. Nguyen, *Advanced Functional Materials*, 2010, **20**, 3314–3321.
58. C. Hu, Y. Fu, S. Li, Z. Xie, and Q. Zhang, *Polym. Chem.*, 2012, **3**, 2949–2955.

RSC Advances Accepted Manuscript

 This journal is © The Royal Society of Chemistry 2012